

Hydrogen-Based Direct Reduction of Iron Oxides Pellets Modeling

Pasquale Cavaliere,* Angelo Perrone, Debora Marsano, and Vito Primavera

The present study deals with the analyses of the direct reduction kinetics during the hydrogen reduction of industrial iron oxide pellets. Various types of pellets with different percentage of total iron content and metal oxides are examined. They are reduced at different temperatures and pressure (700–1100 °C and 1–6 bar) in hydrogen atmosphere. The reduction behavior is described in terms of time to reduction, rate of reduction, and kinetics constant. All the obtained results are analyzed through the employment of a commercial multiobjective optimization tool to precisely define the weight that each single parameter has on the reduction behavior. It is shown that from the point of view of the processing conditions, temperature is the main factor influencing the time to total reduction. From the point of view of the pellets properties, it is mainly influenced by the total iron percentage and then by porosity and basicity index. Also, the kinetics behavior is largely influenced by the reduction temperature even if it is mainly governed by the porosity and pores size from the point of view of the reduced pellets. The reduction rate is also mainly influenced by temperature and then by iron percentage, gas pressure, basicity index, and porosity.

Obviously, the process produces 1.8 tons of carbon dioxide per ton of crude steel with a total emissions level of 3.46Gt contributing to the 6.7% of the total anthropogenic emissions. The production levels are destined to increase over and over in the next future and so, the continuous optimization of the traditional routes is not sufficient. As a matter of fact, the reduction of global warming needs fundamental technological reconversions in order to meet strong emissions limitations in the next future.^[1]

In the last decades, direct reduction (DR) represented an affordable innovative process in the ironmaking processing. The most widespread technologies are the Midrex and HYL shaft furnaces accounting for almost 80% of the globally produced direct reduced iron.^[2]

Here, basically, syngas is employed as the main reducing agent with remarkable differences in the plants configuration.^[3]

This is due to the fundamental aspect that various problems can be encountered about the reduction kinetics of iron oxides in the CO–H₂–CO₂–H₂O atmosphere of the shaft furnace.^[4,5] The unwanted kinetics modifications provide higher energy consumptions of the overall ironmaking processing.^[6,7] A comprehensive understanding of the role of the reducing gas composition and temperature on the process is of significance to achieve an appropriate reduction efficiency and product quality.^[8] Depending on the reducing atmosphere and temperature, the performance of the technology, such as the reduction rate, metallization degree, and behavior of the iron ore, varies significantly.^[9]

From a scientific point of view, this leads to several complications in the development of a robust model capable of providing affordable results in the prevision of the reduction behavior of direct reduced pellets.^[10]

For these reasons, the most available models in the literature take into consideration the reduction through a gas mixture of hydrogen and carbon monoxide in order to simplify the thermochemical and thermophysical phenomena involved in the process development.^[11,12]


In the direct reduction process, the reducing agent converts the iron ore to elemental iron directly. The final product is directly reduced iron (DRI) including matrix elements from the ore. Typical feed gases for direct reduction are either hydrogen or natural gas with methane (CH₄) as the main constituent. The generation of this gas occurs through methane reforming, which can be done in a reformer or inside the reduction shaft

1. Introduction

Ironmaking and steelmaking are facing significant evolutions in the recent past. The traditional integrated route is characterized by considerable environmental impacts due to materials handling, energy issues, and direct emissions. In 2020, the global steel production accounts for 1869 million tons (Mt) where the traditional blast furnace–basic oxygen furnace covers the 70% of the overall crude steel. The world situation by the main producer countries is shown in **Figure 1**.

P. Cavaliere, A. Perrone, D. Marsano
Department of Innovation Engineering
University of Salento
Via per Arnesano, 73100 Lecce, Italy
E-mail: PASQUALE.CAVALIERE@UNISALENTO.IT

V. Primavera
EnginSoft S.p.A.
Zona Industriale, Via Antonio Murri 2, Mesagne, 72023 Brindisi, Italy

 The ORCID identification number(s) for the author(s) of this article can be found under <https://doi.org/10.1002/srin.202200791>.

© 2023 The Authors. Steel Research International published by Wiley-VCH GmbH. This is an open access article under the terms of the Creative Commons Attribution License, which permits use, distribution and reproduction in any medium, provided the original work is properly cited.

DOI: 10.1002/srin.202200791

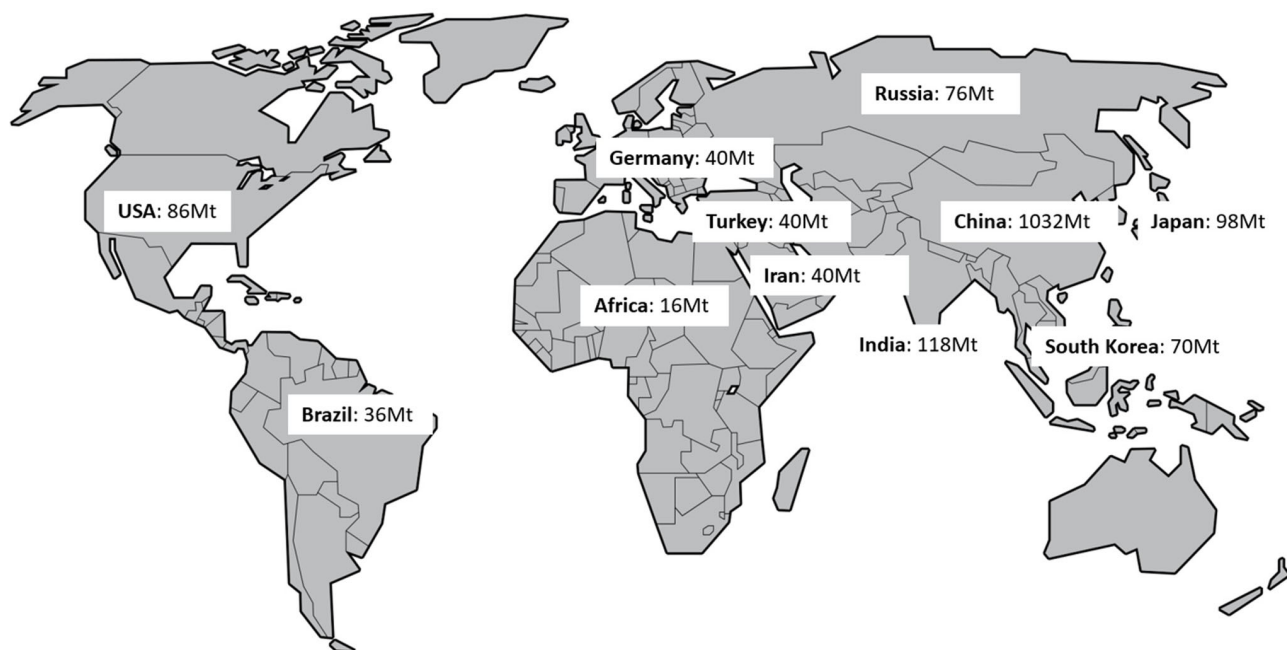


Figure 1. Global ten main steel producers (the picture is provided by considering the data reported in ref. [40]).

with the sponge iron as a catalyst.^[13] The utilization of hydrogen as the reducing agent has the great advantage that gaseous water is the sole by-product.^[14] In this view it is easy to establish the real effect of hydrogen as substitute of carbon monoxide in the direct reduction relating its usage to the carbon consumption and carbon dioxide emissions reduction during ironmaking.^[15] The hydrogen-based direct reduction process includes multiple types of chemical reactions, solid-state and defect-mediated diffusion (of oxygen and hydrogen species), several phase transformations, as well as massive volume shrinkage and mechanical stress buildup.^[16] The volume expansion of the pellets is inevitable during the reduction, and the abnormal swelling would cause serious accidents, such as poor permeability, even collapse of the burden.^[17]

The hydrogen-based process is characterized by a complex chemomechanical interplay of the different mechanisms involved, specifically the underlying reactions, mass transport, and volume changes.^[18] Among the reaction steps, wüstite reduction to iron is the slowest one by nearly an order of magnitude lower reaction kinetics compared with the other two steps; therefore, it plays an important role in determining the overall rate of the reactions.^[19]

Now, many analytical models can be found in the literature in order to predict the kinetics behavior of direct reduction as a function of the many factors influencing the overall process.^[20] These factors are mainly the gas mixing, the reactor temperature and pressure, and the pellet solid properties (dimensions, porosity, pores size, tortuosity, and mineralogy).^[9] Given this large quantity of very different factors, the uncertainty results sometimes very high.

For this reason, the main approach is based on a balancing between the model simplicity and its accuracy that is related to the agreement with the experimental data.^[21]

Anyway, the scientific interest about the reduction process through hydrogen has rapidly grown in the very recent past. This is also driven by industry where the continuously increasing cost of the reformed natural gas becomes crucial for the production of sponge iron.

This has become fundamental because the kinetics of direct reduction is directly related to the production rate of the massive process.^[22,23] As a matter of fact, the relationships among the pellet conditions, the gaseous environment, and the final product properties are far to be firmly established. From a scientific point of view, the results are absolutely not conclusive.

As a general way, the reduction rates are greater in the case of hydrogen employment and remarkably lower in the case of carbon monoxide environment with intermediate results (not linearly defined) in the case of intermediate percentages of the two gases.^[24] This is directly correlated with the fact that the small molecular diameter of hydrogen allows for the acceleration of the reduction reactions. Another simple aspect is that as the temperature of the atmosphere increases the kinetics of the process is accelerated.^[25] In the case of employment of gas mixtures, the kinetics increases as the temperature and the hydrogen content in the gas mixture increase.^[24]

So, the use of hydrogen as reducing agent is fundamental for the process speed. Anyway, many issues are related to the costs of hydrogen production as well as to the reaction thermodynamic because the hydrogen in the gas mixture allows for endothermic reactions and so larger gas volumes are needed to balance the heat losses.^[26] The reduction of iron oxides with molecular hydrogen is endothermic, whereas carbon monoxide reduction is exothermic. Above 800 °C, however, thermodynamics are more favorable with hydrogen than with carbon monoxide, where the reduction rate with H₂ is much higher than the case with CO at 850 °C.

Now, even if many articles are published on the direct reduction of iron ore fines, no general consensus is reached on the direct reduction kinetics in the case of industrial pellets. Here, the starting composition is very complex because of the raw material origin and many different issues are related to the pelletizing process. So, a deep comprehensive agreement on the weighted contribution of all the factors influencing the reaction kinetics (pellet type, processing condition, and so on) has not been achieved yet. In addition, many discrepancies are noted in the case of employment of different gas mixtures. Another limit of the available information is that many experimental evidences are proposed with experiences performed on just on type of very similar types of industrial pellets.

Another important industrial aspect is that sponge iron generally requires a carbon content in the range 1.5–4.5% that is fundamental for the further melting operations. Now, the pellets reduced via pure hydrogen are carbon free, leading to an increase in the melting temperature of the sponge iron (1538 °C). As a consequence, carburization is needed.^[27] DR under CO atmosphere is often accompanied by carbon deposition due to an inverse Boudouard reaction at temperatures <1000 °C.

From a chemical point of view, direct reduction is one of the best examples of noncatalytic solid–gas reactions. In these kinds of reactions, continuous transient structural changes occur at the solid state as the chemical reactions take place. These structural changes alter the physical behavior of the gas–solid system. All these effects as well as other specific aspects lead to additional complications in the precise analytical description of the reduction process. In this view, the investigation of the main variables affecting the overall reduction process is fundamental for the deep understanding of the involved phenomena.

For the industrial pellets direct reduction, the complexity increases as a consequence of continuous consecutive reduction reactions accompanied with continuous structural transformation of the solid phase as the reduction proceeds.

Now, the rate-controlling step (that can be of chemical, diffusive, or intermediate nature) of the reduction process is not unique. It depends on processing conditions such as temperature, pressure, flow rate, and gas composition as well as on the pellet properties such as size, morphology, porosity, pore size, tortuosity, and chemical composition.^[28] Given all these involved factors, the available experiments are commonly performed by varying just one parameter by taking the other ones constant. In this way, the interaction among all the factors influencing the process is neglected. In addition, many experimental evidences are restricted to limited sets of conditions.

Basically, the reduction of hematite through hydrogen is based on three different reactions involving Fe₂O₃, Fe₃O₄, FeO, and Fe. Here, the rate-controlling step is not only due to chemical reactions presenting different steps with various diffusive limitations for the gas. For this reason, the kinetics analyses based on the fitting of the Arrhenius equation lead to the presentation in the literature of large variability. This limits the general employment of many parameters in the industrial design and applications.

Now, during the reduction of porous iron oxides pellets the following steps can be underlined: 1) mass transfer of the gases (hydrogen, carbon monoxide, or their mixing) from the stream to the pellet surface; 2) initial diffusion of the gas through the film surrounding the pellet; 3) diffusion through the pores of the

reduced layer to the reduction front-oxide layer; 4) adsorption at the oxide interphase; 5) oxygen removal via phase boundary reactions; 6) formation of water vapor and carbon dioxide, iron oxides, and ferrous iron; 7) desorption of gases belonging to the reactions; 8) solid-state diffusion of the reacted products; 9) diffusion of gaseous products back toward the pellet surface; and 10) mass transfer of the gaseous product toward the stream.

Given this, it is intuitive how the pellets porosity largely influences the reduction rate. This is due to the fact that porosity directly influences the gases diffusion.

Obviously, in the case of pellets with low porosity, the reducing gases have difficulties to penetrate inside the pellets bulk. In such a case, different mechanisms such as solid-state diffusion start to be important even if they are several orders of magnitude lower than gas diffusion. So, chemical transformations take place once the gas is adsorbed at the pellet surface.

Obviously, the kinetics of the chemical reactions is a strong function of the temperature. In the case of low-temperature reduction, the chemical reaction becomes the rate-limiting step. At high temperatures, the temperature increase is exponentially related to the reduction rate; this is described by the Arrhenius equation (Equation (1))

$$k = Ae^{-\frac{E_a}{RT}} \quad (1)$$

where k is the kinetic constant, A is the Arrhenius constant, E_a is the activation energy, R is the universal gas constant, and T is the absolute temperature.

If the temperature is increased, the mass transfer starts to become the rate-limiting step. This is due to the fact that the transport of reactants and reactions by-products is slower with respect to the chemical reactions.^[29,30]

Here, the effective diffusion coefficient is influenced by the gas physical properties and by the temperature. As both temperature and hydrogen content are increased, the diffusion coefficient increases. The difference in the diffusivity of hydrogen and carbon monoxide is due to the difference in the molecules dimensions.

Pressure and its effect on the reduction rate are fundamental. First of all, it should be stated that as the hydrogen content in the gas increases, pressure should be increased because of the higher volatility of hydrogen with respect to the carbon monoxide. If the pressure is increased with the maintaining of the partial pressure of hydrogen, a remarkable effect on the kinetics increase is not recorded especially in the first stages of reduction. On the contrary, the increase in the partial pressure of hydrogen leads to significant high rates of reduction.

Another fundamental aspect is that the pellets do not consist only of iron oxides but also of other oxides, gangue, and impurities. Obviously, the reduction rate is largely influenced on the oxides percentage and on their type. The oxides are typically CaO, TiO₂, SiO₂, Al₂O₃, MnO, and MgO. The reduction rate is increased if the alumina content is less than 3%. These oxides give the so-called basicity index normally evaluated as the rate CaO/SiO₂.^[31]

Another important aspect is that porosity tends to increase as the reduction processes proceed. This phenomenon tends to lead to an acceleration of the reaction kinetics as the reduction process advances.

Given that the diffusion can be the rate-limiting step, porosity and pores dimensions have a remarkable influence on the reduction process. This is due to the fact that both porosity and pores size influence the specific area of the pellets and then define the available surface for the reactions development. This aspect is crucial and must be precisely defined in a model that would soundly describe the evolution of these systems.

Porosity and tortuosity factor are fundamental properties of the pellets. They influence the diffusion of gases; as a matter of fact, as the pore diameter increases (at fixed level of total porosity), molecular diffusion is predominant. Porosity and tortuosity depend on the pelletizing procedure. Pelletizing influences the reduction rates; as a matter of fact, tortuosity influences the gas diffusion. Its values can vary in the range 1–10 even if the main pelletizing procedures allow to obtain tortuosity in the range 1–4.

When the pores tortuosity increases, the gas diffusion becomes more turbulent. In this way, the reduction rate decreases as the tortuosity factor increases.^[32]

The aim of the present article is the description of the kinetics behavior during the hydrogen-based direct reduction of industrial pellets by precisely defining the weight that each single processing, physical, and chemical parameter has on the overall process development.

2. Experimental Procedure

The data employed for the database were obtained from the literature and from our in lab experiments.

The temperature of the furnace was in the range 700–1100 °C. The gas composition was 100% H₂. The gas pressure was varied in the range 1–6 bar. The pellet diameter was in the range 1–20 mm. The total iron in the pellet was in the range 57–70%. The basicity index of the pellets varied from 0 to 2.15. The porosity of the pellets was in the range 15–54%. The pore size varied from 6 to 20 μm and the tortuosity factor from 1 to 10.

The corresponding output was obviously the reduction curves. For the database construction, they were recorded the final carbon percentage in the pellet (obviously in those materials reduced in the presence of carbon monoxide), the kinetic constant, and the rate of reduction.

The kinetic constant was calculated through the 3D diffusion model (Equation (2))

$$k = \frac{[1 - (1 - \alpha)^{\frac{1}{3}}]^2}{t} \quad (2)$$

and through the 3D phase boundary controlled reaction (Equation (3))

$$k = \frac{1 - (1 - \alpha)^{\frac{1}{3}}}{t} \quad (3)$$

where α is the fraction reacted (0–1) and t is the time at which a given fraction of the material reacts.^[33]

The rate of reduction was evaluated through Equation (4) and (5)

$$\frac{dR}{dt_{40}} = \frac{33.6}{t_{60} - t_{30}} \quad (4)$$

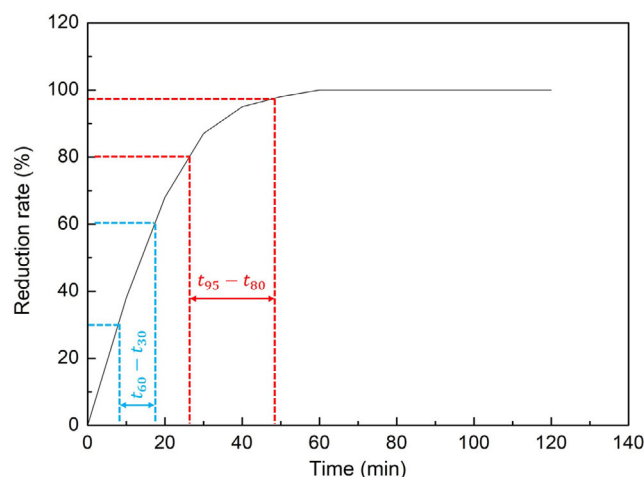


Figure 2. Schematic procedure for the calculation of the rates of reduction.

$$\frac{dR}{dt_{90}} = \frac{13.9}{t_{95} - t_{80}} \quad (5)$$

where t_{95} , t_{80} , t_{60} , and t_{30} is the time required to reduce the pellets by 95, 80, 60% and 30%, respectively, as schematically shown in **Figure 2**.

The employed databases are attached as supplementary material.

2.1. Modeling Procedure

The employed multidisciplinary and multiobjective software is written to allow easy coupling to any computer-aided engineering (CAE) tool. It enables the pursuit of the so-called “Pareto Frontier”: it is the best trade-off between all the objective functions. The advanced algorithms within can spot the optimal results, even conflicting each other or belonging to different fields. The more accurate the analysis is, the more the complexity of the design process increases. modeFRONTIER platform allows the managing of a wide range of software and an easy overview of the entire product development process. modeFRONTIER’s optimization algorithms identify the solutions which lie on the trade-off Pareto Frontier: none of them can be improved without prejudicing another. In other words, the best possible solutions are the optimal solutions. An attempt to optimize a design or system where there is only one objective usually entails the use of gradient methods where the algorithms search for either the minimum or the maximum of an objective function, depending on the goal. One way of handling multiobjective optimization is to incorporate all the objectives (suitably weighted) in a single function, thereby reducing the problem to one of single objective optimization again. This technique has the disadvantage, however, that these weights must be provided a priori, which can influence the solution to a large degree. Moreover, if the goals are very different in substance (e.g., cost and efficiency), it can be difficult, or even meaningless, to try to produce a single all-inclusive objective function.

True multiobjective optimization techniques overcome these problems by keeping the objectives separate during the

optimization process. It should be kept in mind that in cases with opposing objectives there will frequently be no single optimum because any solution will be a compromise. The role of the optimization algorithm is then to identify the solutions which lie on the trade-off Pareto Frontier. These solutions all have the characteristic that none of the objectives can be improved without prejudicing another.

The progresses of high-performance computing offer the availability of accurate and reliable virtual environments to explore several possible configurations. In real-case applications, it is not always possible to reduce the complexity of the problem and obtain a model that can be solved quickly. Usually, every single simulation can take hours or even days. In these cases, the time to run a single analysis makes running more than a few simulations prohibitive and some other smart approaches are needed. These factors lead to a Design of Experiment (DoE) technique to perform a reduced number of calculations. After that, these well-distributed results can be used to create an interpolating surface. This surface represents a meta-model of the original problem and can be used to perform the optimization without computing any further analyses.

Once data have been obtained, whether from an optimization or DoE, or from data importation, the user can turn to the extensive postprocessing features in modeFRONTIER to analyze the results.^[34,35] The software offers wide-ranging toolbox, allowing the user to perform sophisticated statistical analysis and data visualization. It provides a strong tool to design and to analyze experiments; it eliminates redundant observations and reduces the time and the resources to make experiments. DoE is a methodology that maximizes the knowledge gained from an experimental campaign. DoE is generally used in two ways. First of all, the use of DoE is extremely important in experimental settings to identify which input variables most affect the experiment

being run. As it is frequently not feasible in a multivariable problem to test all combinations of input parameters, DoE techniques allow the user to extract as much information as possible from a limited number of test runs. However, if the engineer's aim is to optimize his design, he will need to provide the optimization algorithm with an initial population of designs from which the algorithm can "learn." In this setting, the DoE is used to provide the initial data points.

Exploration DoEs are useful for getting information about the problem and about the design space. They can serve as the starting point for a subsequent optimization process, or as a database for response surface (RS) training, or for checking the response sensitivity of a candidate solution. The system has been successfully applied to many processes during ironmaking and steelmaking.^[36–38]

Starting from a database built with experimental results, computational models were developed (virtual *n*-dimensional surfaces) able to reproduce at best the actual process. The method used for the creation of meta-models to simulate the actual process through the use of physical laws with appropriate coefficients to be calibrated was that of the RS. This method consists of creating *n*-dimensional surfaces that are "trained" on the basis of actual input and output. These surfaces trained on a large experimental data can give the output numbers that reflect the real process. The experimental design consists of almost 1500 inputs and outputs obtained from experimental data. To train the virtual surface in the training phase, they included 1540 experimental design inputs and outputs. We used the remaining in the design validation phase.

The reduction process through the analysis performed by modeFRONTIER is summarized in the workflow of **Figure 3**.

The workflow is divided into data flow (solid lines) and logic flow (dashed lines) that have the computer node as their common

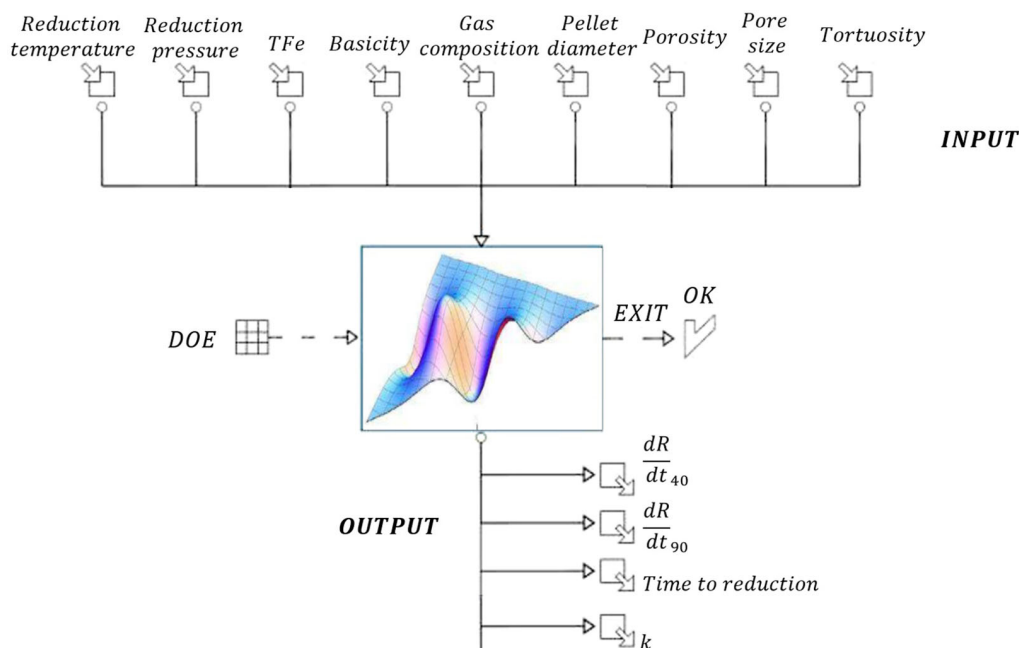


Figure 3. Workflow of analysis describing the input–output correlation.

node. Here, physical and mathematical functions representing the reduction process are introduced. In the data flow, all input parameters optimized in the numerical simulations are included as follows: 1) reduction temperature, 2) reduction pressure, 3) total iron percentage in the pellet (TFe), 4) basicity index, 5) pellet diameter, 6) pellets porosity, 7) pores size, 8) tortuosity factor, and those outputs: 1) kinetic constant (k), 2) reduction rates (from Equation (4) and (5)), 3) time to 100% reduction.

The output variables define a multigoal analysis and have been minimized taking into account some constraints or limitations typical of the actual process. At this stage, the nodes that make up the logic flow of numerical analysis are defined.

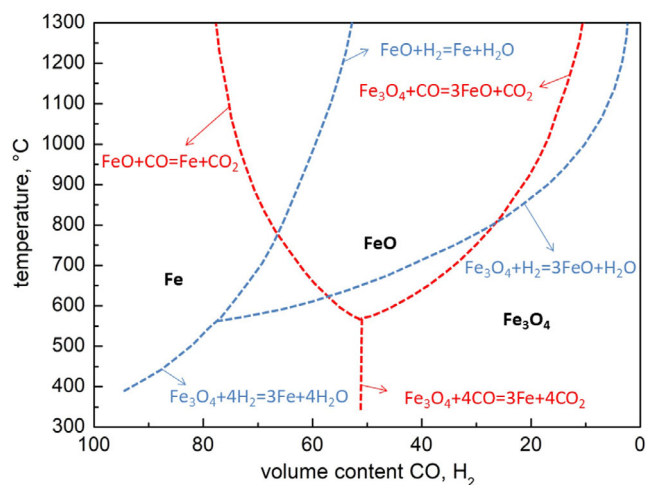


Figure 4. Equilibrium curves for the iron evolution in different CO and H₂ atmospheres.

The first node is the DoE, which is the set of different designs reproducing different possible working conditions. It means creating a set number of designs that will be used by the scheduler (the node where the best algorithm is introduced) for the optimization. Depending on how this space is filled, the designs, defined by the scheduler, are more or less truthful. Therefore, the choice of the DoE is to be assessed correctly. In this phase, the software allows to evaluate the weight that each single input parameter has on the behavior of a given analyzed output. This can be visualized through the so-called scatter matrix where if the weight is zero it means that there is no correlation between a single input and the analyzed output. On the contrary, if the weight is one, there is a total direct correlation between the input and the analyzed output; while if the weight is minus one, this means that there is a total inverse correlation between the input and the analyzed output. Obviously, the intermediate values indicate the relative weight of each single input with direct or inverse correlation if the factor is positive or negative respectively.

Generally, in this kind of analysis, the heart of the optimization is represented by a series of equations of chemical and physical nature of a given resolution to get the desired output. In the present case, all this information is not clear, due to the complexity of the process and so it was chosen to employ the methodology of RS. Optimization software allows the following of different kinds of RS. For each output variable to be minimized, it is necessary to create a response surface. The analysis starts from a database built with data of operating conditions of the reduction plants obtained from experimental measurements. The database is built by introducing the input parameters, the corresponding output for each working condition, and the physical correlations between the different conditions.

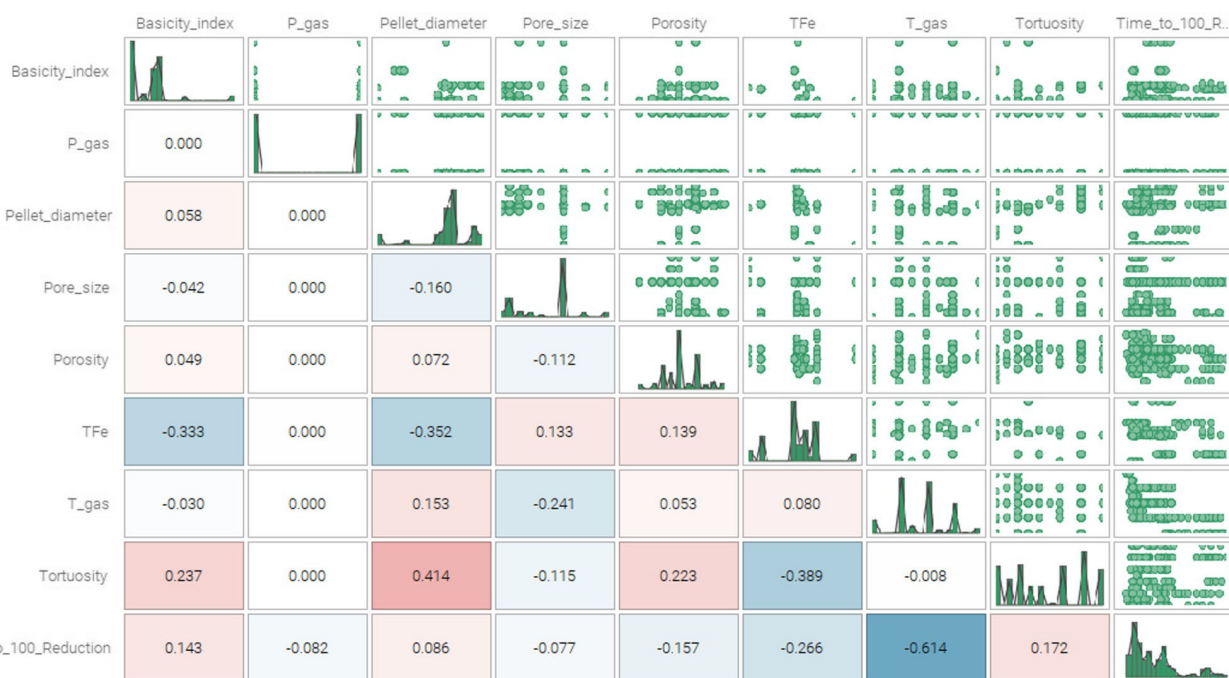


Figure 5. Scatter matrix for the calculation of time to reduction in hydrogen.

3. Results and Discussion

By employing hydrogen in the reduction, diffusivity and chemical reactions rate increase as the temperature increases. The increase in the reduction rate constant as the temperature increases is amplified as the hydrogen content in the mixing increases. As a matter of fact, while the reduction of iron oxide with H_2 and CO has been extensively studied, the kinetics of reduction with H_2 -CO mixtures has not been adequately investigated for a large range of H_2 content. The theoretical behavior of the different iron oxides in the different reducing atmospheres is shown in **Figure 4**.

The change in the ratio of reducing gases has a little impact on the rate of thermal entropy generation. On the other hand, as increasing the ratio of hydrogen to carbon monoxide, the entropy

generation rate decreases as a consequence of the complex interaction between the chemical potential, temperature, and mole fraction. In the case of entropy generation by mass transfer, the entropy generation rate shows small increases as the hydrogen percentage increases. Also, in the case of the coupling of heat and mass transfer, the effect of hydrogen addition is low. As a summary, by increasing the amount of hydrogen in the gas mixture, entropy generation is first decreased and then experiences a peak and finally approaches a constant value with a moderate slope.

As a matter of fact, let's see the scatter matrix relative to the reduction performed through 100% of hydrogen (**Figure 5**).

Here, the time to reduction is mainly influenced by the gas temperature and total iron content in the pellet (with inverse proportionality), as shown in **Figure 6**.

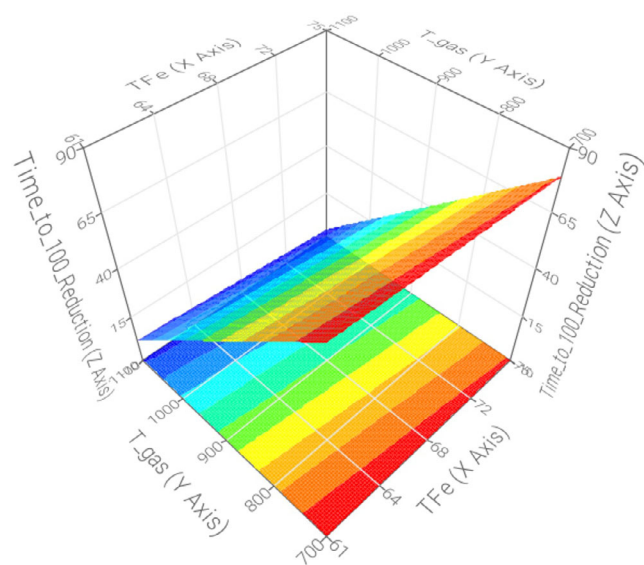


Figure 6. Time to reduction as a function of iron percentage in the pellet and gas temperature in hydrogen atmosphere.

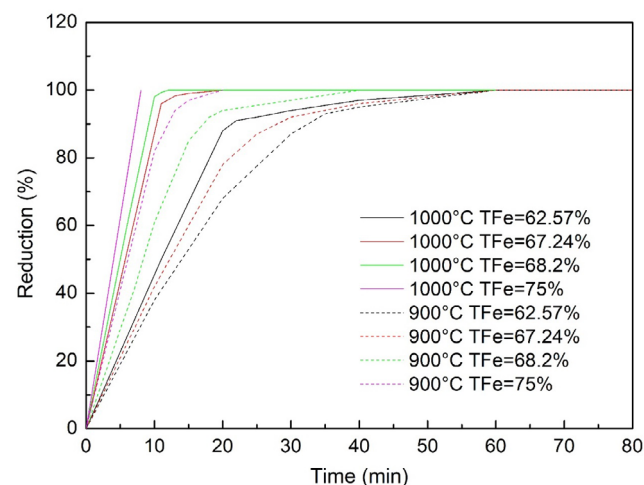


Figure 7. Reduction versus time for different pellets at 900 and 1000 °C of the gas temperature.

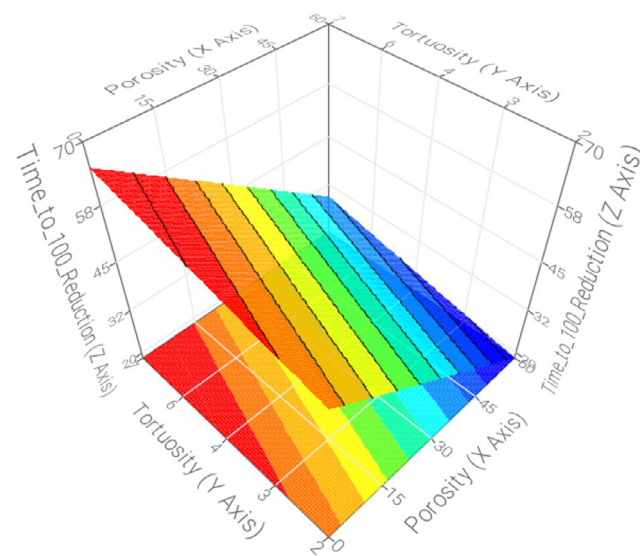


Figure 8. Time to 100% reduction as a function of porosity and tortuosity in hydrogen atmosphere.

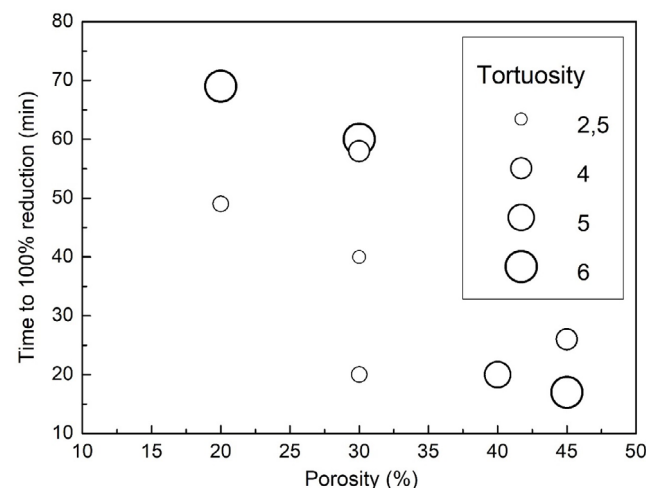


Figure 9. Time to 100% reduction as a function of porosity for different pores tortuosity at the temperature of 1000 °C.

To show the reduction behavior as a function of temperature and iron content in the pellets, **Figure 7** illustrates the reduction behavior versus time of reduction for different reducing temperatures and iron contents.

This is a common aspect for the industrial pellet for direct reduction. In fact, high-quality pellets are generally required for two main reasons. The first one is the final properties of the reduced material that improves the further processing operations as the total iron content increases. This leads to more steel produced with the same tons of treated raw materials. The second is that the time to reduction of high-quality pellets tends to be reduced, so leading to an increase in the shaft furnaces productivity and to the reduction of energy consumption.

In the case of reduction with 100% of hydrogen, the time to complete reduction is directly proportional to the pore tortuosity and inversely proportional to the porosity level and to the pores size (**Figure 8**).

The time to 100% reduction as a function of different porosity levels is shown in **Figure 9**.

As expected, time to reduction decreases as porosity increases and increases at the same level of porosity as the pores tortuosity increases.

Porosity favors the diffusion of gases inside the pellet by accelerating the reduction reactions and leading to reduced times of the process. In general, in the case of high porosity pellets, the gas easily penetrates the particle and reduces all the surfaces at the same time. In the case of high porosity, the pellets dimension has low impact on the overall reduction process. On the contrary, if the pellets have low porosity, the reactions evolve stepwise and they are better described by a shrinking core model. In this case, the reduction results longer as the pellets dimensions increase. This aspect is well described by **Figure 10**.

That clearly indicates how is the pellets diameter increases the porosity effect is different. If porosity is lower, the effect of pellet diameter is decreased. The contrary happens in the case of larger particles where porosity starts to be more important in the pellets reduction.

Obviously, this is not a constant condition; in fact, if very hard dense iron layers develop during reduction, this strongly lowers

the reduction rate. This is due to the fact that particles cannot be properly penetrated by the reducing gases. In this case, the reduction evolves through solid-state diffusion through the hard layers to continue the iron oxides transformations. This solid-state diffusion is slower and slower with respect to the gaseous diffusion. The penetration through the hard iron layers can be improved through the temperature increase. Anyway, this is a costly procedure and it can lead to large softening of the pellets with a deformation producing porosity decrease and consequently reduction rates lowering.

By considering the tortuosity inside the pellets, in general, the reduction rate increases as the porosity increases and the tortuosity decreases. From an energy point of view, porosity, pores size, and tortuosity represent a large influence on the entropy variations during all the reduction steps. The entropy generation starts in the first minutes of the reduction process and it is mainly due to the heat transfer between the hot gas and the pellets. In general, the rate of entropy generation increases as the porosity and gas ratio decrease. On the contrary, as the tortuosity increases, the entropy generation rate increases. In fact, the tortuosity factor represents an obstacle to the gas flow. So, as the tortuosity increases, the resistance of the pellets against the diffusion of the gas increases. As a consequence, the rate of entropy generation increases and the reduction effect is decreased.

Entropy is generated by heat and mass transfer and chemical reaction. By considering all the different contributions, the entropy generation by heat transfer increases as the porosity decreases. In the first stages of reduction, entropy shows a net increase due to the high-temperature gradient between the hot gas and the pellet. Then, the entropy generation decreases up to a constant value because of decrease of the thermal gradient.

As the porosity increases, the reducing gases find lower resistance for the penetration. In this way, the entropy generation decreases. By considering the entropy generation by chemical reactions, it increases again in the first stages of reduction and then it decreases by reaching a zero value. This entropy generation again increases as the porosity decreases.

By considering the entropy generation by mass transfer, it increases very quickly in the first stages of reduction and then

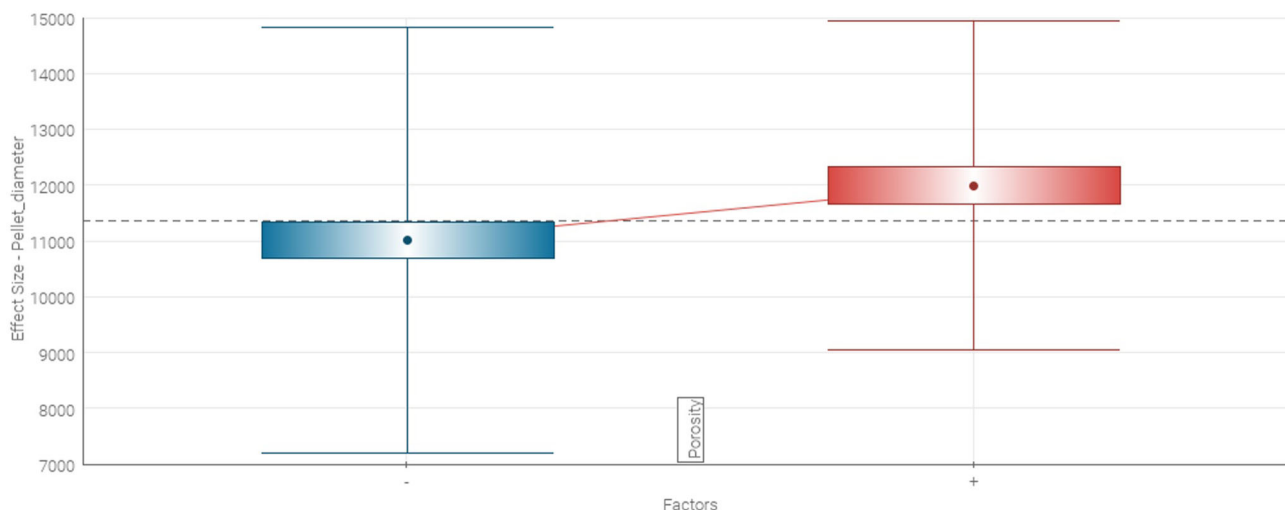


Figure 10. Pellets size effect at different levels of porosity.

it decreases up to a constant value. Here, entropy generation approaches zero faster with increased porosity due to reduced resistance against gas permeation. Even if the iron is totally reduced, the entropy is not null because of an existing mass gradient between the center and the surface of the pellet. Here, again it becomes to be crucial the coupled effect between porosity and pellet diameter influencing the entropy generation and then the reduction behavior. As a matter of fact, the highest contribution to entropy generation is due to the heat transfer, then to the chemical reactions, to the mass transfer, and finally to the coupling between heat and mass transfer.

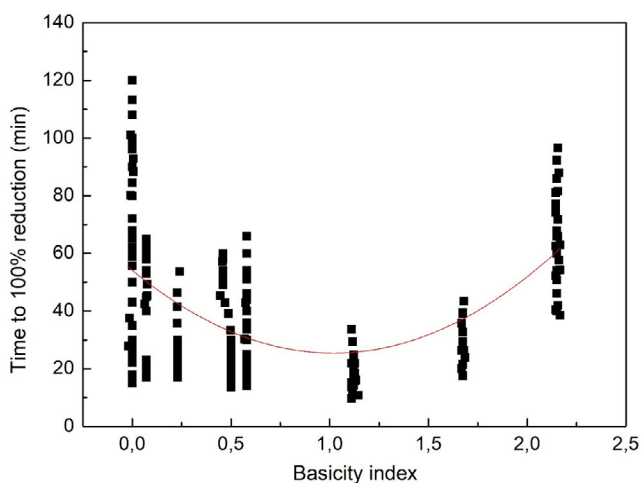


Figure 11. Time to reduction as a function of the basicity index in hydrogen atmosphere.

Another fundamental aspect influencing the reduction behavior is the composition of the pellets in terms of presence of different metal oxides. Here, the basicity index is fundamental in monitoring the effect of these oxides on the reduction of industrial pellets.

A parabolic behavior is underlined in the case of hydrogen reduction for the time to reduction as a function of the basicity index (**Figure 11**).

So again, the reduction behavior of the industrial pellets is related to the quality of the raw material influencing the process and obviously the quality of the final product to be employed for further operations. So, the basicity index should be retained at an appropriate level in order to optimize the reduction process of the pellets. In general, this is more pronounced in the case of further increase of the presence of CaO in the pellets composition. This, in addition, can lead to excessive brittleness of the produced pellets leading to difficult handling in the further processing operations.^[39]

Going toward the effect of the processing parameters on the kinetics constant behavior, the hydrogen-based direct reduction process is characterized by a hierarchy of phenomena that can influence the reaction at different length and time scales. They range from transport and reaction kinetics in a shaft reactor at macroscopic scale down to chemical reactions at interfaces at atomic scale and catalysis, dissociation, and charge transfer at electronic scale. Reaction kinetics is also affected by micro-to-atomic-scale features of the different oxides and the adjacent iron layers, including crystal defects, porosity, mechanics, and local composition. It should be underlined that by adding also small amounts of CO to the hydrogen reducing gas, the diffusion coefficient drastically decreases. However, the kinetic rate constant does not decrease the same amount. The explanation for this

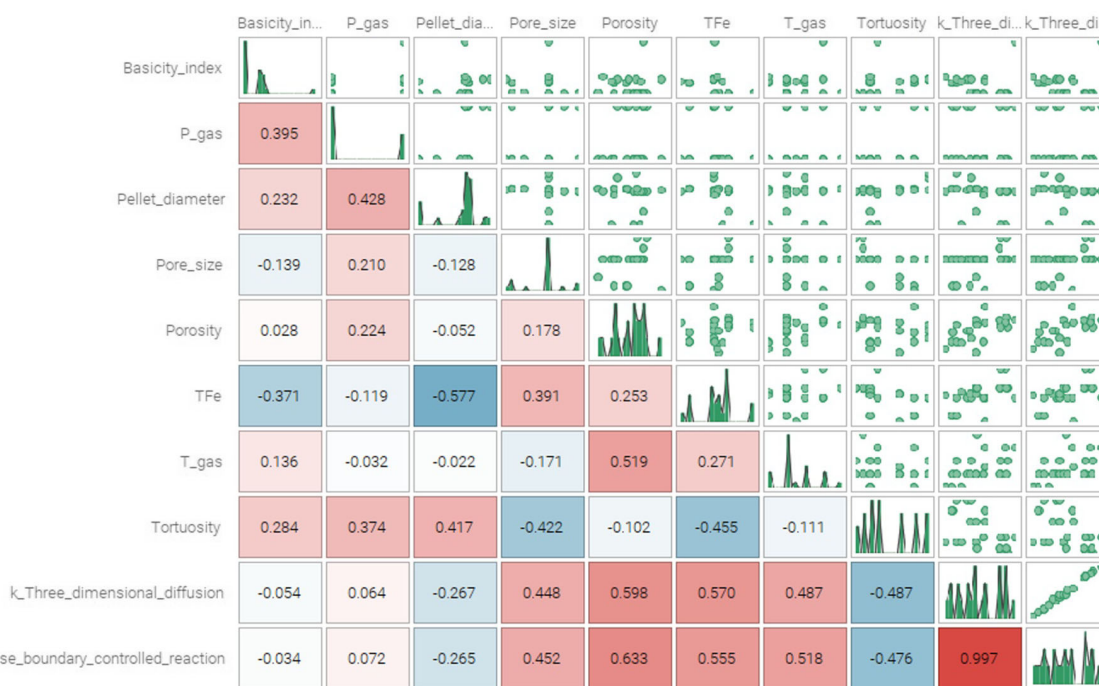


Figure 12. Scatter matrix relative to the kinetics constants in hydrogen.

could be that it only takes a small amount of CO molecules to lower the fluidity of the gas and block the diffusion path, due to the higher viscosity and molecular size of CO and, thus, holding back H₂ from reducing the iron oxides, while the reaction rate constant is largely unaffected.

So, as a matter of fact, the carbon addition leads to a decrease in the kinetic constant for many processing conditions (selected from the whole database).

The scatter matrix relative to the reduction with 100% hydrogen is shown in **Figure 12**.

They obviously increase with increasing temperature. Then, the *k* values are largely influenced by porosity and iron percentage with a direct proportionality (**Figure 13**).

The data for selected pellets are shown in **Figure 14**.

Here, the basicity index is less influential. Tortuosity is inversely proportional to the kinetic constant while pore size is directly proportional (**Figure 15**).

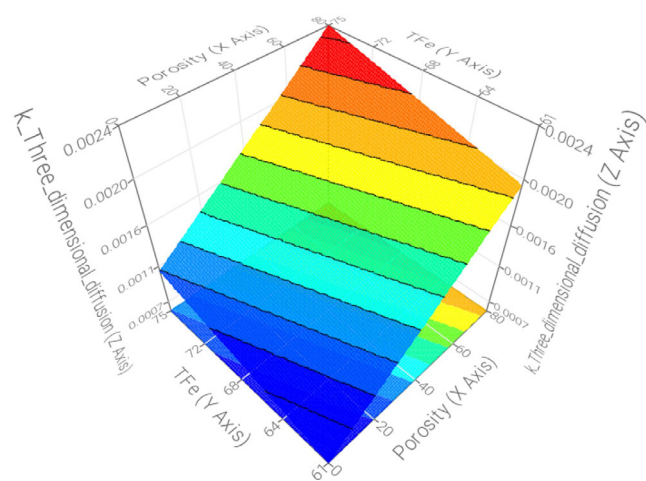


Figure 13. Kinetics constant as a function of iron percentage in the pellet and porosity in hydrogen reducing gas.

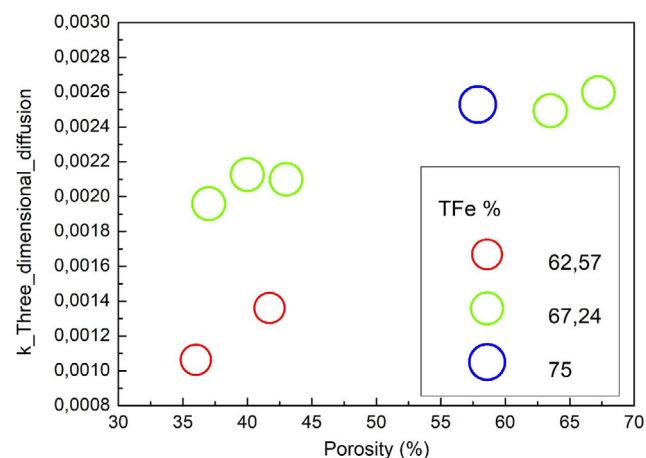


Figure 14. Kinetics constant as a function of porosity for selected percentages of total iron in the pellet.

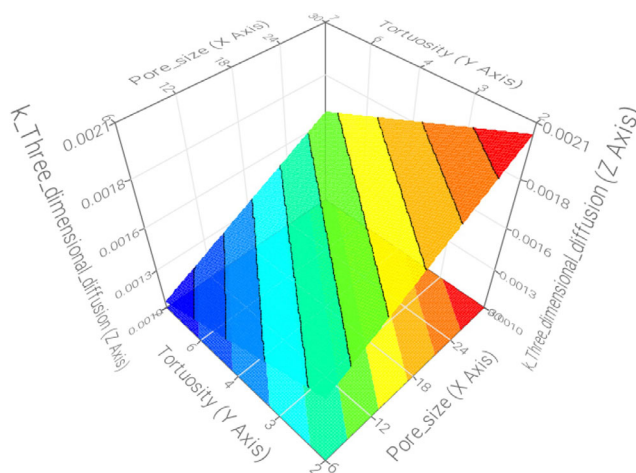


Figure 15. Kinetics constant as a function of tortuosity and pore size.

Tortuosity is a key factor for the kinetics behavior; in fact, in the same conditions of mass transfer, temperature, and pressure, the pellet has less specific atoms of hydrogen to react with the surface as the tortuosity increases. This leads to a remarkable reduction of the kinetics of the process as the tortuosity increases (**Figure 16**).

By analyzing the effect of tortuosity, here the entropy generation by heat transfer is not influenced by this pellet property. The entropy generation by chemical reaction increases as the tortuosity factor increases. The maximum and ultimate rates of entropy generation are increased with increasing tortuosity. Also, in the case of entropy generation by mass transfer, the rate increases as the tortuosity increase. Here, it should be underlined how this contribution largely increases from a tortuosity factor of 3 to a tortuosity factor of 4. By considering all the contributions, the net entropy generation increases with the increase of the tortuosity factor.

Finally, the hydrogen addition leads to a remarkable increase in the kinetics constants behavior, as shown in **Figure 17**, for all the investigated pellets.

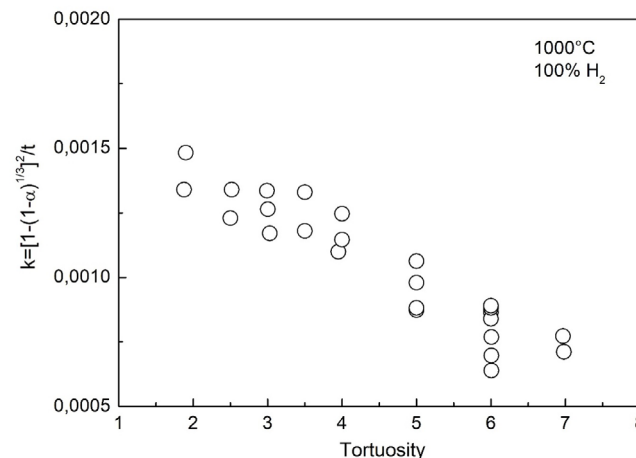


Figure 16. Kinetics constant as a function of tortuosity at 1000 °C reduction in hydrogen.

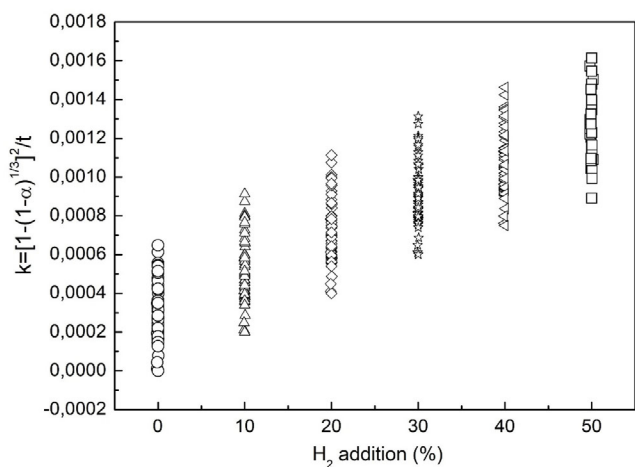


Figure 17. Kinetics constant behavior as a function of the hydrogen percentage.

By analyzing the reduction rates as a function of the pellets properties and the processing parameters, here, the two indexes are differently influenced by the processing conditions because they refer to different zones of the reduction curves where different transformations of the materials under reduction take place. So, the two employed indexes are indicative of the different oxides forms that are reduced during the process. The different stages of reduction indicate the behavior of different reactions taking place in the pellet, so the absolute values and the influence of the input parameters vary. For example, temperature influences the dR/dt_{90} index by 50% more with respect to the influence on dR/dt_{40} . In this way, the temperature of the reducing gas is much more

important for the final stages of the reduction in order to reach a complete metallization. This is due to the fact that being the temperature the driving force for the diffusion inside the pellets it leads the reducing gas to overcome the already reduced layers in order to reach the bulk of the pellet. Initial pore diameter is more influencing for the first stages of reduction with respect to the final ones. This is mainly due to the fact that pores modify as the reduction proceeds. So, by advancing the reduction the gas further going inside the pellet finds different pores to enter inside the material. The same explanations can be done for the absolute value of the starting pellets' porosity and for the porosity. So, pores geometry and dimensions vary during the reduction and their values are more important for the variation of the dR/dt_{40} index with respect to the dR/dt_{90} one. Here, by coupling the effect of heat and mass transfer, there is an entropy peak of generation and then a decrease in an inverse proportionality with porosity. By considering all the contributions, there is a peak of entropy generation in the first stage of reduction, then a decrease followed by another smaller peak generation, and finally a decrease up to a steady state. This theoretical behavior is very consistent with the experimental data observations.

So, by observing what happens in the case of hydrogen reduction (Figure 18).

dR/dt_{40} is largely influenced by temperature (as expected). Then, it is largely influenced by pore size (with a direct proportionality) and pellet diameter (with inverse proportionality), as shown in Figure 19.

Other influencing inputs are the total iron percentage in the pellet as well as porosity with direct proportionality (Figure 20).

By observing the dR/dt_{90} behavior, it is interesting to immediately underline how it is largely influenced by the dR/dt_{40}

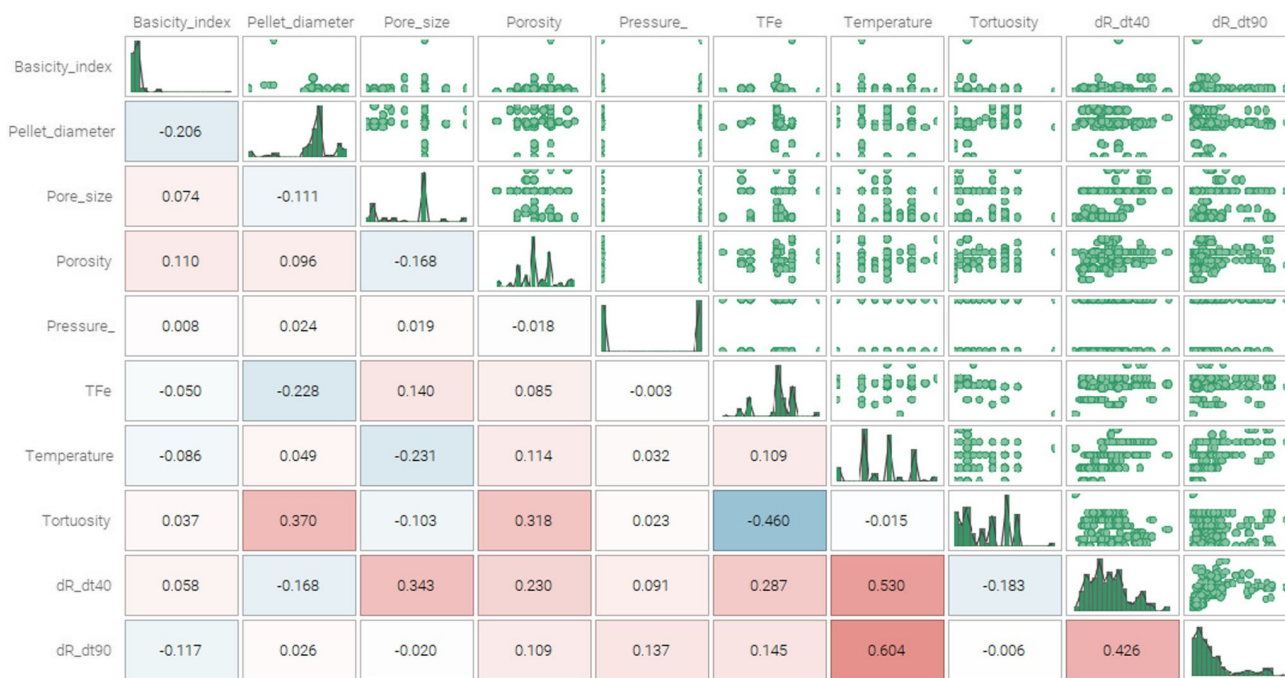


Figure 18. Scatter matrix for the reduction rates in hydrogen.

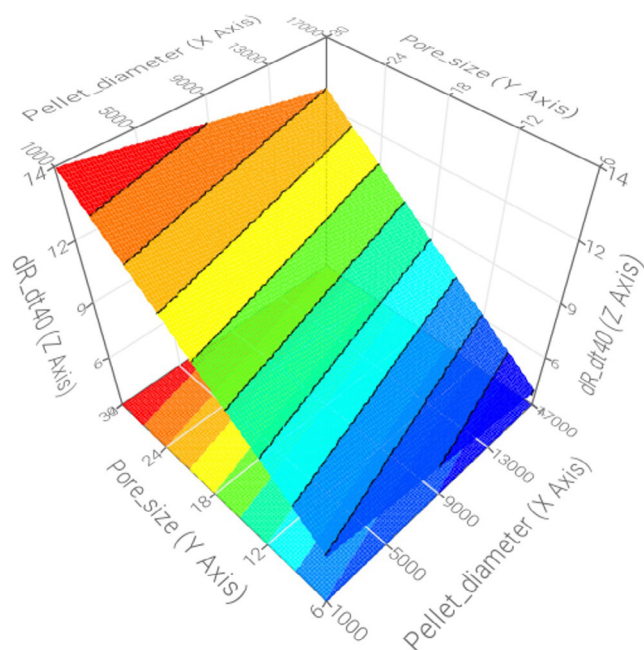


Figure 19. dR/dt_{40} as a function of pore size and pellet diameter.

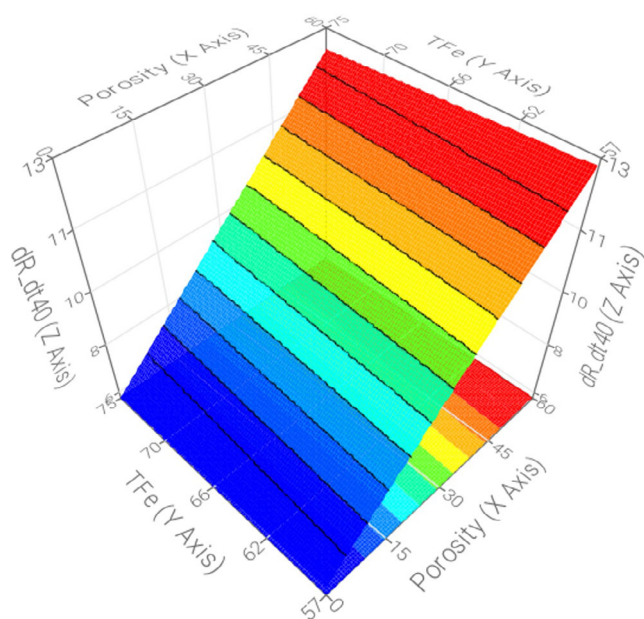


Figure 20. dR/dt_{40} as a function of iron percentage in the pellet and porosity.

behavior; this is very consistent with the present analyses. Then, temperature has a larger influence on this parameter with respect to the rate indicated by the index dR/dt_{40} . On the other hand, the initial porosity seems to be uninfluential and this is due to the fact that pores largely modify during the first stages of reduction. As expected, both basicity index and gas pressure start to be more influential as the reduction continues (Figure 21).

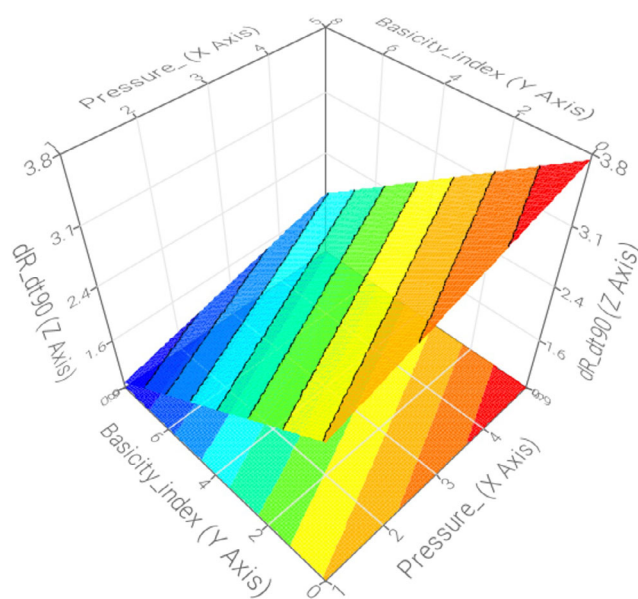


Figure 21. dR/dt_{90} as a function of pressure and basicity index.

Given all these results, it appears very clear how both the processing conditions and the pellets properties have different and large influences on the reduction process. It was largely known that temperature is, in almost all the cases, the main driver for the reduction kinetics. Obviously, the reduction time and the reduction kinetics for the reduction of the different iron oxides forms are largely accelerated in the case of gas employment in the reducing atmosphere by reaching the maximum efficiency for 100% of hydrogen. What results from the present results is that the pellets properties such as composition, porosity, and pores geometry have a very important influence on the kinetics behavior even if the weight of each single property is much or more influential as the processing conditions vary. In addition, this aspect is much more pronounced in the case of reduction performed by mixing carbon monoxide and hydrogen in the reducing gas. This happens because the physical parameters are largely related to both the atmosphere properties and the gas diffusion behavior at given levels of temperature and pressure.

4. Conclusions

The aim of the present article was to present the evolution of the direct reduction of iron oxide industrial pellets with different physical and chemical properties. The reduction behavior evolution was analyzed as a function of the processing parameters settled during the process. The main calculated results were the time to reduction of the pellets, the kinetic constants, and the rates of reduction. All the obtained data were analyzed by employing a multiobjective optimization tool capable of providing the weight that each single parameter has on the resulting output. The employed system allowed also to correlate the most influencing parameter to a given output. A general conclusion that can be underlined is that, by varying the composition of the reducing

gas, the influence of the different input parameters largely changes from the point of view of both processing parameters and chemical–physical properties of the reduced pellets. The reduction through total hydrogen shows the fastest reduction behavior with total time to reduction mainly influenced by the temperature and by the chemical properties of the employed industrial pellets. In the case of hydrogen reduction, the kinetic constants are mainly influenced by the pellets porosity, pore size, and tortuosity. In terms of reduction rates, during hydrogen processing, the calculated indexes show a very complex behavior related to the pellets properties and porosity because of the material evolution underlined during the different stages of reduction. The rate of reduction is largely influenced by the chemical–physical properties of the pellets as well as by the porosity conditions.

Supporting Information

Supporting Information is available from the Wiley Online Library or from the author.

Acknowledgements

Open Access Funding provided by Universita del Salento within the CRUI-CARE Agreement.

Conflict of Interest

The authors declare no conflict of interest.

Data Availability Statement

The data that support the findings of this study are available from the corresponding author upon reasonable request.

Keywords

direct reduction, entropy, hydrogen, kinetics, metallization degree, processing parameters

Received: October 14, 2022

Revised: December 22, 2022

Published online: March 18, 2023

- [1] P. Cavaliere, *Clean Ironmaking and Steelmaking Processes Efficient Technologies for Greenhouse Emissions Abatement*, Springer, Cham, Switzerland **2019**, <https://doi.org/10.1007/978-3-030-21209-4>.
- [2] I. R. Souza Filho, H. Springer, Y. Ma, A. Mahajan, C. Cau'e da Silva, M. Kulse, D. Raabe, *J. Clean. Prod.* **2022**, *340*, 130805.
- [3] D. Guo, L. Zhu, S. Guo, B. Cui, S. Luo, M. Laghari, Z. Chen, C. Ma, Y. Zhou, J. Chen, B. Xiao, M. Hu, S. Luo *Fuel. Proc. Technol.* **2016**, *148*, 276.
- [4] M. S. Valipour, M. Y. Motamed Hashemi, Y. Saboohi, *Adv. Powder Technol.* **2006**, *17*, 277.
- [5] E. A. Mousa, A. Babich, D. Senk, *Steel Res. Int.* **2013**, *84*, 1085.
- [6] A. Ranzani da Costa, D. Wagner, F. Patisson, *J. Clean. Prod.* **2013**, *46*, 27.
- [7] Y. Zhang, Q. Yue, X. Chai, Q. Wang, Y. Lu, W. Ji, *J. Clean. Prod.* **2022**, *361*, 132289.
- [8] C. Scharm, F. Küster, M. Laabs, Q. Huang, O. Volkova, M. Reinmoller, S. Guhl, B. Meyer, *Miner. Eng.* **2022**, *180*, 107549.
- [9] M. Kazemi, M. S. Pour, D. Sichen, *Metall. Met. Trans.* **2017**, *B48*, 1114.
- [10] P. Metolina, T. R. Ribeiro, R. Guardani, *Int. J. Miner. Metall. Mater.* **2022**, *29*, 1908.
- [11] T. R. Ribeiro, J. B. Ferreira Neto, J. G. Rocha Poco, C. Takano, L. Kolbeinsen, E. Ringdalen, *ISIJ Int.* **2022**, *62*, 504.
- [12] S. Geng, H. Zhang, W. Ding, Y. Yu, *Metalurgija* **2018**, *57*, 219.
- [13] T. R. Ribeiro, J. B. Ferreira Neto, J. G. Rocha Poco, C. Takano, L. Kolbeinsen, E. Ringdalen, *ISIJ Int.* **2021**, *61*, 182.
- [14] A. Loder, M. Siebenhofer, A. Bohm, S. Lux, *Clean. Eng. Technol.* **2021**, *5*, 100345.
- [15] P. Cavaliere, *Hydrogen Assisted Direct Reduction of Iron Oxides*, Springer, Cham, Switzerland **2021**, <https://doi.org/10.1007/978-3-030-98056-6>.
- [16] Y. Bai, J. R. Mianroodi, Y. Ma, A. Kwiatkowski da Silva, B. Svendsena, D. Raabe, *Acta Mater.* **2022**, *231*, 117899.
- [17] Z. Zhao, J. Tang, M. Chu, X. Wang, A. Zheng, X. Wang, Y. Li, *Int. J. Miner.* **2022**, *29*, 1891.
- [18] S. Li, H. Zhang, J. Nie, R. Dewil, J. Baeyens, Y. Deng, *Sustainability* **2021**, *13*, 8866.
- [19] Y. Ma, I. R. Souza Filho, Y. Bai, J. Schenk, F. Patisson, A. Beck, J. A. van Bokhoven, M. G. Willinger, K. Li, D. Xie, D. Ponge, S. Zaefferer, B. Gault, J. R. Mianroodi, D. Raabe, *Scr. Mater.* **2022**, *213*, 114571.
- [20] M.-H. Bai, H. Long, S.-B. Ren, D. Liu, C.-F. Zhao, *ISIJ Int.* **2018**, *58*, 1034.
- [21] A. Z. Ghadi, M. S. Valipour, S. M. Vahedi, H. Y. Sohn, *Steel Res. Int.* **2020**, *91*, 1900270.
- [22] N. A. El-Husseiny, A. El-Amir, F. M. Mohamed, S. T. Abdel-Rahim, M. E. H. Shalabi, *Int. J. Sci. Eng. Res.* **2015**, *6*, 1018.
- [23] E. M. Abdel Hamid, S. K. Amin, H. A. Sibak, M. F. Abadir, *Int. J. Appl. Eng. Res.* **2018**, *13*, 3954.
- [24] M. L. Ali, Q. Fradet, U. Riedel, *Steel Res. Int.* **2022**, *93*, 2200043.
- [25] Y. Ma, I. R. Souza Filho, X. Zhang, S. Nandy, P. Barriobero-Vila, G. Requena, D. Vogel, M. Rohwerder, D. Ponge, H. Springer, D. Raabe, *Int. J. Miner. Metall. Mater.* **2022**, *29*, 1901.
- [26] P. Cavaliere, A. Perrone, A. Silvello, *Metals* **2021**, *11*, 1816.
- [27] P. Cavaliere, A. Perrone, A. Silvello, P. Stagnoli, P. Duarte, *Metals* **2022**, *12*, 203.
- [28] A. A. El-Geassy, M. I. Nas, *ISIJ Int.* **1990**, *30*, 417.
- [29] Q. Fradet, M. L. Ali, U. Riedel, *Steel Res. Int.* **2022**, *93*, 2200042.
- [30] H.-B. Zuo, C. Wang, J.-J. Dong, K.-X. Jiao, R.-S. Xu, *Int. J. Miner. Metall. Mater.* **2015**, *22*, 688.
- [31] Y. Shi, D. Zhu, J. Pan, Z. Guo, S. Lu, M. Xu, *Powder Technol.* **2022**, *408*, 117782.
- [32] A. Zare Ghadi, M. S. Valipour, M. Biglari, *IJE Trans. B: Appl.* **2018**, *31*, 1274.
- [33] Y. Man, J. Feng, *Powder Technol.* **2016**, *301*, 674.
- [34] P. Cavaliere, A. Perrone, A. Silvello, *Eng. Sci. Technol.* **2016**, *19*, 292.
- [35] P. Cavaliere, A. Perrone, A. Silvello, *J. Manuf. Proc.* **2015**, *17*, 9.
- [36] P. Cavaliere, A. Perrone, *Steel Res. Int.* **2013**, *85*, 89.
- [37] P. Cavaliere, A. Perrone, *Ironmaking Steelmaking* **2013**, *40*, 9.
- [38] P. Cavaliere, A. Perrone, P. Tafuro, V. Primavera, *Ironmaking Steelmaking* **2011**, *38*, 422.
- [39] G.-C. Zhang, G.-P. Luo, P.-F. Jia, Y.-C. Wang, Y.-F. Chai, *High Temp. Mater. Proc.* **2021**, *40*, 193.
- [40] <https://worldsteel.org/wp-content/uploads/2021-World-Steel-in-Figures.pdf> (accessed: August 2022).